Materials Physics and Mechanics 47 (2021) 159-169 Received: September 9, 2020

BALLISTIC RESISTANCE OF CERAMIC METALLIC TARGET FOR VARYING LAYER THICKNESSES

M.K. Khan[1], M.A. Iqbal[1*], V. Bratov[2], N.F. Morozov[2,3], N.K. Gupta[4]

[1]Department of Civil Engineering, Indian Institute of Technology Roorkee, Roorkee-247667, India

[2]Institute for Problems in Mechanical Engineering, Russian Academy of Sciences, Saint Petersburg, Russia

[3]Department of Theory of Elasticity, Saint Petersburg State University, Saint Petersburg, Russia

[4]Department of Applied Mechanics, Indian Institute of Technology Delhi, New Delhi-110016, India

*e-mail: iqbal_ashraf@rediffmail.com

Abstract. The ballistic behaviour of a bi-layer ceramic-metal target against steel projectile with varying layer thicknesses has been investigated using a three-dimensional finite element model. The bi-layer target was made of alumina 99.5 % ceramic front layer and aluminium 2024-T3 metallic back layer with an areal dimension of 100×100 mm and the thickness of both layers were varied, with the total thickness of the composite being kept as 10 mm and 20 mm. A steel 4340 cylindrical blunt-nosed projectile was used with 30 grams mass and 10.9 mm diameter. The Johnson-Holmquist 2 (JH-2) constitutive model was used for reproducing the high strain behavior of alumina and Johnson-Cook (JC) model was used for aluminium alloy and steel. The impact velocity of the projectile was varied in the range 200-700 m/s for 10 mm total thickness and 500-800 m/s in the case of 20 mm total thickness for studying the effects of thickness ratios on ballistic resistance of the bi-layer target. The residual velocities were compared and the ratio of front to back layer providing the highest ballistic limit velocity was found for both cases.

Keywords: Ballistic resistance, Ceramic-metallic target, ballistic limit velocity

1. Introduction

The behaviour of ceramic under large deformation and high strain rate loading has been extensively studied for its application in protective structures. The ceramic is widely used in composite armours due to its higher compressive strength, higher hardness, and lower density. In case of a ballistic impact, the ceramic layer shatters and erodes the high-velocity incoming projectile leading to distortion of the nose and drop in the momentum of the projectile. The ceramic based composite armour has its primary application as protective layers in mobile structures like vehicles, aircraft, and body armour, where lightweight is a prime requirement [1].

When the projectile impacts the ceramic layer of the composite target, the ceramic is broken instantly. The functional utility of the metallic layer in composite armour is to support the ceramic fragments and absorbing the remaining kinetic energy of the projectile while undergoing plastic deformation. The alloys of aluminium have lesser weight density and are commonly used as backing material having sufficient tensile strength to support ceramic layer during a ballistic impact. The ballistic resistance capacity of alumina based bi-layer composite target with different aluminium alloys as the backing layer was varied significantly at lower velocities when impacted by steel 4340 blunt cylindrical projectile. The performance of

http://dx.doi.org/10.18149/MPM.4722021_1

alumina backed by four different aluminium alloys; namely 1100-H12, 6061, 2024-T3 and 7075 was being compared. The bi-layer target with aluminium alloys 7075 backing layer shows the best ballistic resistance. The ballistic resistance of bi-layer target was found to be lower in the case of aluminium alloy 6061 backing layer in comparison of alloy 2024 and 1100 backing layer although 6061 alloy has higher yield strength than alloy 2024 and 1100. The performance of the bi-layer target was found to be not showing dependence only on the yield strength of the backing material [2]. The tensile strength and hardness of aluminium 2024 were reported to be increased with heat treatment leading to superior ballistic performance of alumina-aluminium composite target against 7.62 mm AP projectiles. The addition of cover plate by reducing the thickness of other components to maintain a constant thickness reduces the ballistic efficiency of a composite target. The alumina-aluminum bi-layer target was found to be having higher ballistic resistance for the ratio of front layer alumina to back layer aluminium lying in the range of 1-3 [3]. The depth of penetration in an aluminium block of 100 mm cube with alumina layer protection and without alumina layer protection was compared against high velocity impact of steel spheres of 6.35 mm diameter. The alumina layer of 4 mm thickness backed by 2 mm aluminium layer was provided with a gap of 30 mm in front of aluminum cube. The depth of penetration was always found to be lesser for alumina layer protected block. The weight saving for the same level of protection with alumina layer protection was higher for impact velocities under 1800 m/s. The diameter of the damage zone in the aluminium block was measured and found to be higher in the case of alumina protection due to the shattering of the projectile after interaction with the ceramic layer. The brittle nature of the projectile leads to lesser depth of penetration for incidence velocities higher than 1800 m/s for aluminium block without alumina protection [4]. The ballistic behaviour of 100 mm square alumina (Al_2O_3) target of 5 mm thickness without any back layer was investigated against the impact of steel 4340 ogival projectile of 10.9 mm shank diameter. The velocity of the impacting projectile was achieved in a range of 52-275 m/s. The damage area in ceramic was found to be increasing and ceramic fragment size was found to be decreasing with the increase in incidence velocity of the projectile. The damage in the projectile and ceramic target was found to be increased in the case of oblique impact of 15º and 30º obliquity [5]. The diameter to length ratio (D/L) of a steel 4340 projectile was varied while maintaining constant mass to study the effects of D/L ratio on the ballistic behaviour of a bi-layer alumina-aluminium target. The bi-layer target attained higher ballistic limit velocity against projectiles having higher D/L ratios [6]. The properties of metallic backing layer as mentioned like tensile strength, hardness, and nature of impacting projectile and ratio of the front layer to back layer effects the performance of a bi-layer target. The thickness ratios of the front layer to the back layer is found to be of paramount importance for design optimization in terms of weight, for providing desired level of protection at minimum possible weight. The optimization of thickness of layers in terms of constant total thickness involves the determination of the ratio providing maximum ballistic limit velocity for a given total thickness of a composite target.

In the present study, a finite element three-dimensional model has been developed to compare the ballistic behaviour of alumina 99.5% and aluminium 2024-T3 composite target of varying layer thickness ratios. The optimum ratio of front to back layer thickness for a constant total thickness has been achieved. Two cases of 10 mm total thickness and 20 mm total thickness of the target have been considered. The residual velocities for three different ratios have been compared for both cases.

2. Constitutive Models

The Johnson-Holmquist-2 (JH-2) model has been used for brittle ceramic and Johnson-Cook (JC) model has been applied for metallic projectile and back layer for reproducing their behaviour under ballistic load.

Johnson-Holmquist-2 (JH-2). The JH-2 [7] model proposed by Johnson and Holmquist has been widely used for modelling the behaviour of ceramic under loading conditions resulting in high strain rate, large deformation, and high pressure and high stress [6,8-9]. The model gives the equivalent strength related to pressure and damage, see Fig. 1. The normalized equivalent stress for strength:

$$\sigma^* = \sigma_i^* - D\left(\sigma_i^* - \sigma_f^*\right) \quad (1)$$

Where, σ_i^* and σ_f^* are normalized intact and fracture strength, D is the damage varying between 0 for intact material and 1 for fully fractured material. The equivalent stresses are normalized by dividing the value by the equivalent stress value at Hugoniot elastic limit (HEL). The HEL is the net compressive stress corresponding to the uniaxial strain (shock wave) exceeding the elastic limit of the material. The HEL contains both the pressure and deviator stress components [10].

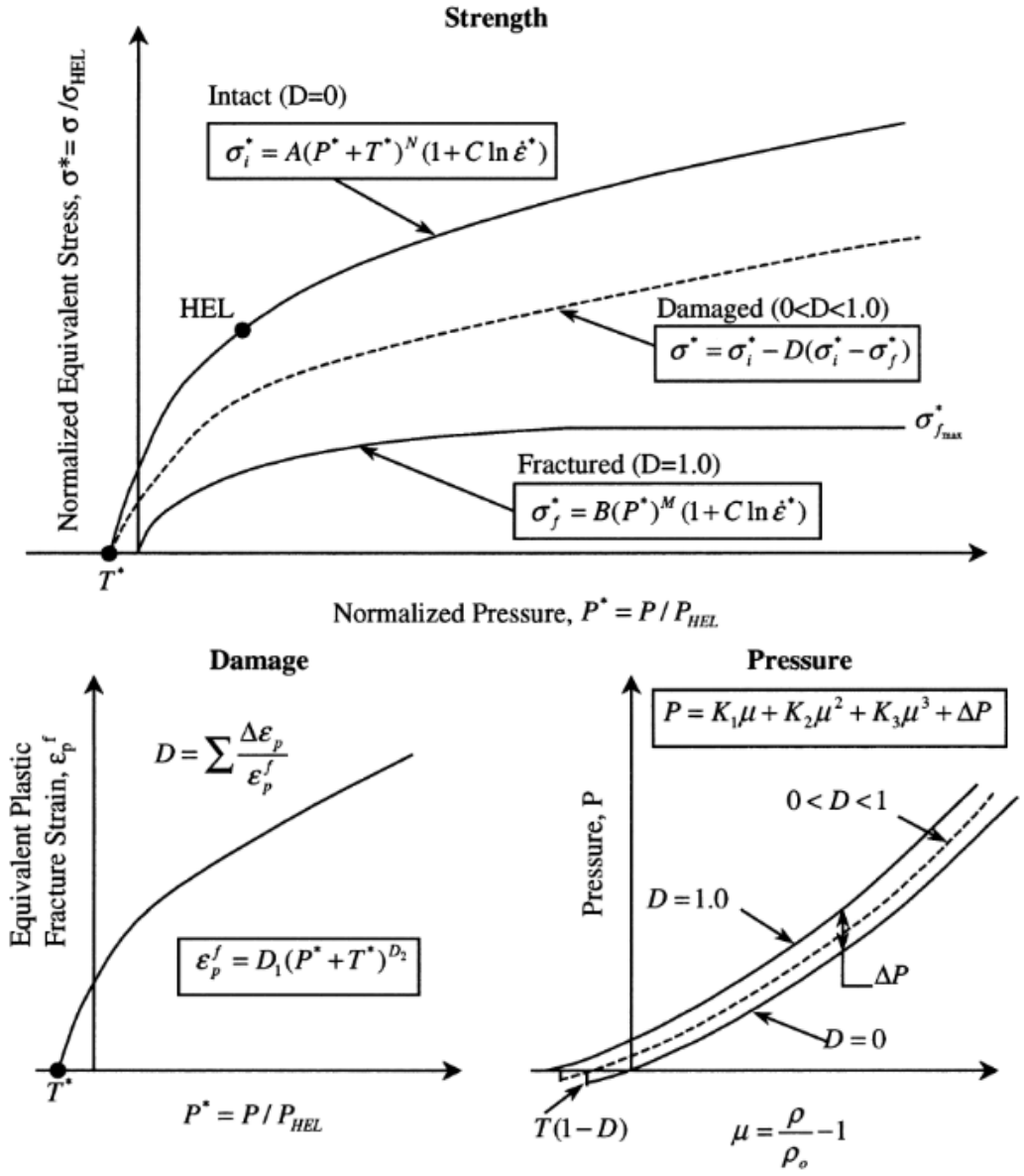

Fig. 1. The JH-2 Model [10]

The intact and fracture strength are:

$$\sigma_i^* = A(P^* + T^*)^N(1 + C \ln \dot{\varepsilon}^*) \quad (2)$$

$$\sigma_f^* = B(P^*)^M(1 + C \ln \dot{\varepsilon}^*) \quad (3)$$

Where, $A, B, C, M,$ and N are the material constants. The normalized pressure P^* is the actual pressure divided by pressure at HEL; whereas normalized maximum tensile hydrostatic pressure T^* is the maximum tensile hydrostatic pressure the material can withstand divided by pressure at HEL. The dimensionless strain rate $\dot{\varepsilon}^*$ is the actual equivalent strain rate divided by reference strain rate. The damage for fracture accumulated in the JH-2 model as:

$$D = \sum \frac{\Delta \varepsilon_p}{\varepsilon_p^f}, \quad (4)$$

where $\Delta \varepsilon_p$ is the equivalent plastic strain during a cycle of integration and is ε_p^f the plastic strain to fracture, calculated as:

$$\varepsilon_p^f = D_1(P^* + T^*)^{D_2}, \quad (5)$$

where D_1 and D_2 are the damage constants. The pressure is related to volumetric strain (μ) before and after damage accumulations are:

$$P = K_1\mu + K_2\mu^2 + K_3\mu^3, \quad (6)$$

$$P = K_1\mu + K_2\mu^2 + K_3\mu^3 + \Delta P, \quad (7)$$

where K_1, K_2 and K_3 are pressure constants, and K_1 is the bulk modulus of the material. The material parameters have been taken from [5], see Table 1. The parameters determination of a material needs extensive work consisted of experiments at high strain rate and high pressure and exhaustive numerical study [10].

Table 1. JH-2 constitutive model parameters for alumina 99.5% [5]

Material parameters	**Numerical values**
Density (kg/m^3)	3700
EOS	**Polynomial**
Bulk modulus, K_1 (GPa)	130.95
Pressure constant, K_2 (GPa)	0
Pressure constant, K_3 (GPa)	0
Strength model	**JH-2**
Shear modulus, G (GPa)	90.16
Hugoniot elastic limit (HEL) (GPa)	19
Intact strength constant, A	0.93
Intact strength exponent, N	0.6
Strain rate constant, C	0
Fracture strength constant, B	0.31
Fracture strength exponent, M	0.6
Normalized maximum fractured strength	1
Pressure at HEL (GPa)	1.46
Failure model	**JH-2**
Damage constant, d_1	0.005
Damage exponent, d_2	1
Bulking factor, β	1

Johnson-Cook (JC). The behaviour of aluminium backing layer and steel 4340 projectile under the impact load have been modelled using the Johnson-Cook (JC) elasto-viscoplastic material model [11-12]. The JC model has been used for aluminium [13-14] and steel [15-16] under large deformations at high strain rate loading in the available literature.

The JC model is used for modelling the flow and fracture behaviour of metals incorporating the effects of material yielding, plastic flow, isotropic strain hardening, strain rate hardening, and thermal softening. The equivalent von Mises stress $\bar{\sigma}$ represented as:

$$\bar{\sigma} = \{A + B(\bar{\varepsilon}^{pl})^n\}\left\{1 + C\ln\left(\frac{\dot{\bar{\varepsilon}}^{pl}}{\dot{\varepsilon}_0}\right)\right\}\{1 - \hat{T}^m\}, \tag{8}$$

where A, B, n, C and m are the material parameters. $\bar{\varepsilon}^{pl}, \dot{\bar{\varepsilon}}^{pl}$ $\dot{\varepsilon}_0$ are equivalent plastic strain and the equivalent plastic strain rate and a reference strain rate. $\hat{T}$ is the non-dimensional temperature:

$$\hat{T} = \begin{cases} 0 & \text{for } T < T_0 \\ \frac{(T - T_0)}{(T_{melt} - T_0)} & \text{for } T_0 \le T \le T_{melt} \\ 1 & \text{for } T > T_{melt} \end{cases} \tag{9}$$

where T_0 is the transition temperature and T_{melt} is the melting point temperature. The damage is accumulated in a similar manner as discussed in JH-2 model, see Eqn. (4). The equivalent plastic strain at failure represented as a function of stress-triaxiality, strain rate, and adiabatic effects:

$$\bar{\varepsilon}_f^{pl} = \left[D_1 + D_2 exp\left(D_3 \frac{\sigma_m}{\bar{\sigma}}\right)\right]\left[1 + D_4 ln\left(\frac{\dot{\bar{\varepsilon}}^{pl}}{\dot{\varepsilon}_0}\right)\right][1 + D_5\hat{T}], \tag{10}$$

where $D_1 - D_5$ are the material damage parameters. The determination of all the parameters of JC model has been discussed in detail in Iqbal et al. [16]. The JC model parameters for aluminium 2024-T3 and steel 4340 are given in Table 2 [6].

Table 2. The parameters of JC Model [6]

Constants with units	**Al 2024-T3**	**Steel 4340**
Density (Kg/m^3)	2785	7770
EOS	Shock	Linear
Strength Model	JC	JC
Shear Modulus, G (GPa)	26.92	77
Static Yield Strength, A (GPa)	0.167	0.950
Strain Hardening Constant, B (GPa)	0.596	0.725
Strain Hardening Exponent, n	0.551	0.375
Strain Rate Constant, C	0.001	0.015
Thermal Softening Exponent, m	0.859	0.625
Melting Temperature, K	893	1793
Reference Strain Rate	1	1
Failure Model	JC	JC
Damage Constant, D_1	0.112	-0.8
Damage Constant, D_2	0.123	2.1
Damage Constant, D_3	1.5	-0.5
Damage Constant, D_4	0.007	0.002
Damage Constant, D_5	0	0.61

3. Validation

The experimental data of a previous study was used for the validation of the numerical model developed in the present study [5]. The alumina 99.5% ceramic with 95×95 mm areal clear

span and 5 mm thickness was impacted on by steel 4340 ogival nosed projectiles of 10.9 mm shank diameter and 30 grams mass. The residual velocity was reported to be 153 m/s corresponding to an incidence velocity of 215 m/s. The numerical simulation model developed in the present study gave the residual velocity of 151 m/s with a minor error of only 1%. The mode of failure of ceramic was also closely matched. Henceforth, the model developed was found to be giving rational predictions.

4. Numerical Model

The finite element simulations have been performed on ABAQUS/Explicit finite element code employing validated JH-2 and JC model for the target and the projectile material. The alumina 99.5% with a planar dimension of 95 × 95 mm has been used with varied thickness. The alumina is backed by aluminium 2420-T3 layer of 95×95 mm planar dimension. The interaction between both the layers has been provided as general contact with the kinematic contact algorithm having a coefficient of friction 0.5. The projectile has been taken as a 10.9 mm diameter cylinder with length 46 mm, weighing equivalent to 30 grams. The interaction between the projectile and centre zone of the target was modelled using the surface to surface contact with kinematic contact algorithm assuming negligible friction due to high velocity of the projectile and small thickness of the target.

The target was restrained with respect to translation and rotation at the peripheral edges. A typical model of the target with and without meshing is shown in Fig. 2, showing the meshing style and boundary conditions. The central portion of the target of size 50 mm × 50 mm is provided with linear C3D8R elements of size 0.6 mm × 0.6 mm × 0.6 mm, while the remaining portion of the plate was modelled using 1 mm × 1 mm × 1 mm sized linear C3D8R elements. The linear C3D8R elements of size 0.6 mm × 0.6 mm × 0.6 mm were used for the meshing of the projectile.

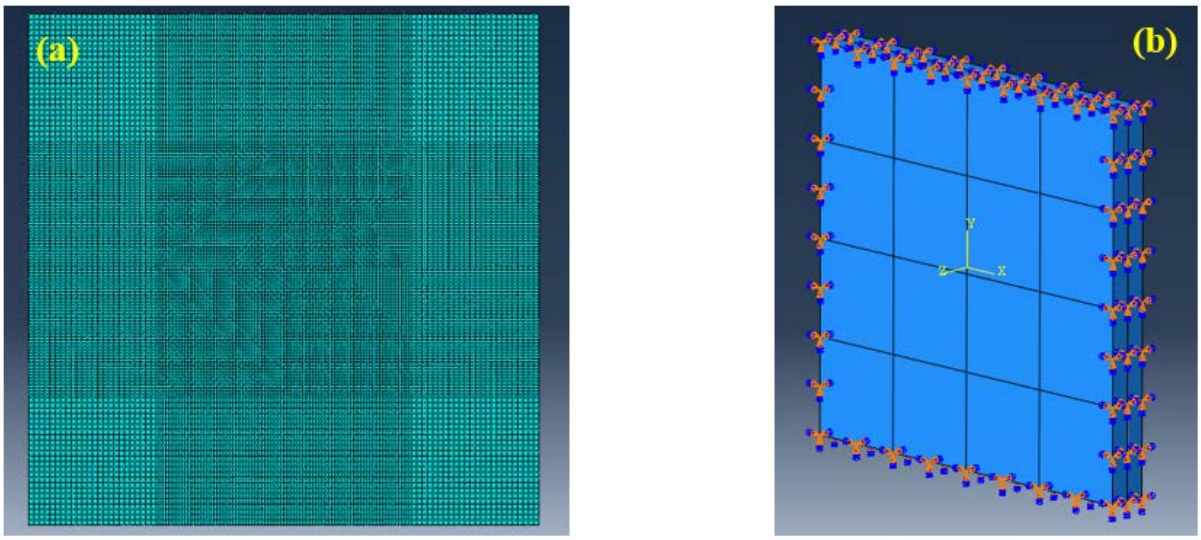

Fig. 2. The typical target (a) Meshing of the target (b) restrained against all degrees of freedom at the edges

Six cases of different thickness of the layers have been investigated in the present study, see Table 3. The total thickness of bi-layer composite target has been taken as 10 mm and 20 mm. Three ratios of front layer to back layer thickness (1, 1.5 and 2.3) were considered for both 10 mm and 20 mm thickness. The least thickness ratio of front layer to back layer has

been taken equivalent to unity as the ballistic resistance of a bilayer target reduced significantly for the ratio of front layer to back layer thickness less than unity [17].

Table 3. The different configuration based on ratio of front layer to back layer thickness

S. No.	Cases	Front layer thickness (mm)	Back layer thickness (mm)	Ratio of front layer to back layer
1	10R1	5	5	1
2	10R2	6	4	1.5
3	10R3	7	3	2.3
4	20R1	10	10	1
5	20R2	12	8	1.5
6	20R3	14	6	2.3

5. Results and discussions

The bi-layer alumina-aluminium target has been impacted by 10.9 mm diameter cylindrical blunt projectile with incidence velocity ranging, 200-700 m/s for 10 mm total thickness and 500-800 m/s for 20 mm total thickness. When the projectile impacts the ceramic front layer, the ceramic gets comminuted in front of the projectile, and cracks are initiated and propagates in the ceramic. The fracture conoid is formed in the ceramic layer by the interaction of radial and circumferential cracks. The load is transferred to the backing layer through this fracture conoid. The remaining energy of the projectile is dissipated by plastic deformation of the backing layer. As the stresses in the backing layer reaches to failure stress of the metallic backing layer, the plugging occurs, see Fig. 3.

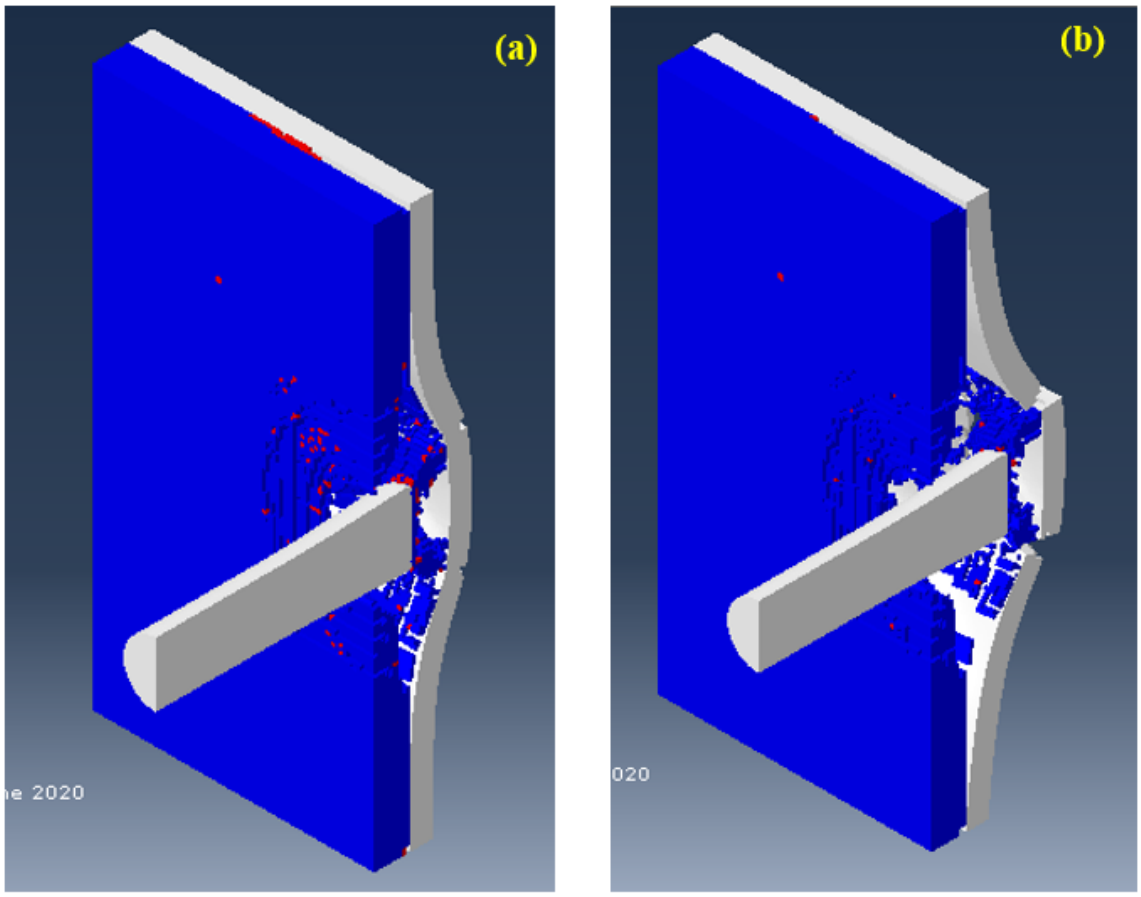

Fig. 3. The failure mechanics of 10R1 configuration (a) 40 μs (b) 80 μs when impacted with an 300 m/s incidence velocity

The residual velocities have been compared for three cases of the different front layer to back layer thickness ratios, see Table 4. At the incidence velocity of 200 m/s the 10R1 ratio gave the best performance with the lowest residual velocity among the three cases. In the variation of incidence velocities from 300 to 700 m/s with an interval of 100 m/s, the 10R2 configuration seems to perform better with lesser residual velocities among the three cases. Although, the difference in the residual velocities is of very small order but overall best ballistic performance was found for the 10R2 configuration in terms of residual velocities.

Table 4. The residual velocities of the projectile at different incidence velocities for three cases of varying front to back layer thickness ratio

S. No.	Incidence Velocity (m/s)	Residual Velocity (m/s)		
		10R1	10R2	10R3
1	200	27	46	45
2	300	170	168	163
3	400	259	253	255
4	500	342	335	342
5	600	439	426	444
6	700	532	518	521

The variation in the ballistic limit velocity is also found to be very small. The ballistic limit velocity is worked out as the average of lowest incidence velocity with complete perforation and the highest incidence velocity with no perforation. The ballistic limit velocities are presented in Table 5. The best performance in terms of ballistic limit velocity is found to be for 10R1 configuration; the ratio of front layer to back layer thickness is equivalent to unity.

Table 5. The values ballistic limit velocities for 10 mm composite bi-layer target

S. No.	Configuration	Ballistic limit velocity (m/s)
1	10R1	185
2	10R2	175
3	10R3	165

The failure of both the layer in the bi-layer target of 20 mm total thickness is shown in Fig. 4. The failure of the ceramic layer with formation of fracture conoid is evident at 20 μs and plugging of the back layer aluminium is occurred at 80 μs. The mushrooming of the projectile has also occurred in the initial phase of the interaction of the projectile with the ceramic layer.

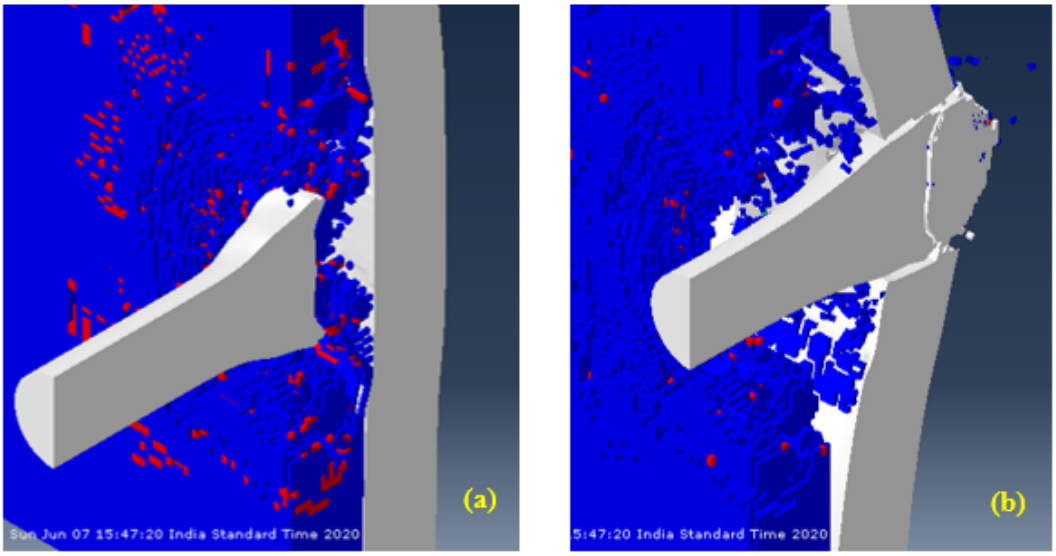

Fig. 4. The failure mechanics of 20R1 configuration (a) 20 μs (b) 80 μs when impacted with an 700 m/s incidence velocity

The residual velocities for 20 mm total thickness have been compared in Table 6. The incidence velocities has been taken in the range, 500-800 m/s, with an interval of 100 m/s. The 20R2 case was found to be having minimum residual velocities among the three ratios. The residual velocities are much higher for both the case 20R1 and 20R2 than 20R2 at relatively lower incidence velocities.

Table 6. The residual velocities of the projectile at different incidence velocities for three cases of varying front to back layer thickness ratio

S. No.	Incidence Velocity (m/s)	Residual Velocity (m/s)		
		20R1	20R2	20R3
1	500	109	0	244
2	600	236	133	298
3	700	295	235	353
4	800	336	321	427

The ballistic limit velocities are given in Table 7. The highest ballistic limit velocity has been achieved in the case of 20R2; the ratio of front layer thickness to back layer thickness was 1.5. The ballistic limit velocity is very close for 20R1 and 20R2, although 20R2 is also found to be giving lesser values of residual velocities for corresponding incidence velocities which means higher level of dissipation of the kinetic energy of the incoming projectile.

Table 7. The values ballistic limit velocities for 10 mm composite bi-layer target

S. No.	Configuration	Ballistic limit velocity (m/s)
1	20R1	490
2	20R2	505
3	20R3	415

The ratio of front layer to back layer thickness giving the highest ballistic limit velocity was found to be 1 and 1.5 for 10 mm and 20 mm total thickness respectively among the three cases considered for both the thicknesses.

6. Conclusion

The variation of ballistic performance of alumina 99.5% ceramic backed by aluminium 2024-T3 with varying thickness of the layers was studied. The thickness of front layer and back layer of the composite target was varied with the total thickness being kept constant at 10 and 20 mm.

Three ratios of front layer to back layer thickness 1, 1.5, and 2.3 were considered. The composite bi-layer target was impacted by blunt-nosed cylindrical steel 4340 projectile.

The residual velocities for three ratios were compared for 10 mm composite target under incidence velocities in the range, 200-700 m/s. The variation in the residual velocities was not very high, although overall 1.5 ratio was giving lesser residual velocities for most of the incidence velocities.

The ballistic limit velocity was found to be highest when the ratio of front layer to back layer thickness was equivalent to unity for 10 mm composite target. Although, the performance of the three cases was not significantly varying in the range of ratios considered.

The 20 mm composite target was impacted with incidence velocities lying in the range, 500-800 m/s. The residual velocities were found to be significantly lesser for 1.5 ratio and also the ballistic limit was highest for this ratio.

The ratio of front layer to back layer thickness giving the highest ballistic limit velocity was found to be varying with the variation in total thickness of the composite target.

Acknowledgements*. Authors gratefully acknowledge the financial support provided by the Department of Science and Technology (DST) India and Russian Foundation for Basic Research (RFBR) Russia through research grant nos. INT/RUS/RFBR/P-232, INT/RUS/RFBR/P361 for successfully carrying out this work.*

References

[1] Bresciani LM, Manes A, Giglio M. An analytical model for ballistic impacts against ceramic tiles. *Ceramics International.* 2018;44(17): 21249-21261.

[2] Venkatesan J, Iqbal MA, Gupta NK, Bratov V, Kazarinov N, Morozov F. Ballistic characteristics of bi-layered armour with various aluminium backing against ogive nose projectile. *Procedia Structural Integrity.* 2017;6: 40-47.

[3] Übeyli M, Yıldırım RO, Ögel B. Investigation on the ballistic behavior of Al2O3/Al2024 laminated composites. *Journal of Materials Processing Technology.* 2008;196(1-3): 356-364.

[4] Hazell PJ, Fellows NA, Hetherington JG. A note on the behind armour effects from perforated alumina/aluminium targets. *International Journal of Impact Engineering.* 19981;21(7): 589-595.

[5] Khan MK, Iqbal MA, Bratov V, Morozov NF, Gupta NK. An investigation of the ballistic performance of independent ceramic target. *Thin-Walled Structures.* 2020;154: 106784.

[6] Khan MK, Iqbal MA, Bratov V, Gupta NK, Morozov NF. A numerical study of ballistic behaviour of ceramic metallic bi-layer armor under impact load. *Materials Physics and Mechanics.* 2019;42(6): 699-710.

[7] Johnson GR, Holmquist TJ. An improved computational constitutive model for brittle materials. *AIP Conference Proceedings* 1994;309(1): 981-984.

[8] Venkatesan J, Iqbal MA, Madhu V. Experimental and numerical study of the dynamic response of B4C ceramic under uniaxial compression. *Thin-Walled Structures.* 2020;154: 106785.

[9] Serjouei A, Gour G, Zhang X, Idapalapati S, Tan GE. On improving ballistic limit of bi-layer ceramic–metal armor. *International Journal of Impact Engineering.* 2017;105: 54-67.

[10] Holmquist TJ, Templeton DW, Bishnoi KD. Constitutive modeling of aluminum nitride for large strain, high-strain rate, and high-pressure applications. *International Journal of Impact Engineering.* 2001;25(3): 211-231.
[11] Johnson GR, Cook WH. Fracture characteristics of three metals subjected to various strains, strain rates, temperatures and pressures. *Engineering Fracture Mechanics.* 1985;21(1): 31-48.
[12] Johnson GR, Cook WH. A constitutive model and data for metals subjected to large strains, high strain rates and high temperatures. In: *Proceedings of the 7th International Symposium on Ballistics.* 1983. p.541-547.
[13] Gupta PK, Iqbal MA, Mohammad Z. Energy dissipation in plastic deformation of thin aluminum targets subjected to projectile impact. *International Journal of Impact Engineering.* 2017;110: 85-96.
[14] Iqbal MA, Tiwari G, Gupta PK, Bhargava P. Ballistic performance and energy absorption characteristics of thin aluminium plates. *International Journal of Impact Engineering.* 2015;77: 1-5.
[15] Senthil K, Iqbal MA. Prediction of superior target layer configuration of armour steel, mild steel and aluminium 7075-T651 alloy against 7.62 AP projectile. In: *Structures.* Elsevier; 2020.
[16] Iqbal MA, Senthil K, Bhargava P, Gupta NK. The characterization and ballistic evaluation of mild steel. *International Journal of Impact Engineering.* 2015;78: 98-113.
[17] Hetherington JG. The optimization of two component composite armours. *International journal of Impact Engineering.* 1992;12(3): 409-414.